Numerical Solution for Supersonic Turbulent Flow over a Compression Ramp

J. S. Shang* and W. L. Hankey Jr.†
Flight Dynamics Laboratory, Wright-Patterson Air Force Base, Ohio

A modified eddy viscosity model is incorporated into the compressible Navier-Stokes equations. The modification attempts to reproduce the response of turbulence to a severe pressure gradient in the flowfield. This relaxation phenomenon is described by an exponential decay of the unperturbed eddy viscosity coefficient downstream of the perturbation in terms of a prescribed length scale. The system of equations is solved by MacCormack's time-splitting explicit numerical scheme for a series of compression corner configurations. Computations are performed for ramp angles varying from 15 to 25° at a Mach number of 2.96 and a Reynolds number of 10^7. Calculations utilizing the modified eddy viscosity for the interacting turbulent flow compare very well with experimental measurements, particularly in the prediction of the upstream pressure propagation and location of the separation and the reattachment points. Good agreement is also attained between the measured and calculated density profiles in the viscous-inviscid interaction region.

Nomenclature

C_f = skin-friction coefficient $2\tau_\omega/\rho_e U^2 e$
D = Van Driest damping factor, Eq. (14)
e = specific energy
e_i = specific internal energy, $c_v T$
F,G = vector fluxes in mean-flow equations
h = maximum vertical dimension of the computational domain
L = length of the leading plate, 1 ft
p = static pressure
q = $u\cos\alpha + v\sin\alpha$
P_r = molecular Prandtl number
P_{r_t} = turbulent Prandtl number
S = distance along the surface
t = time
T = temperature
u,v = velocity components in the Cartesian coordinates
$U_{\max}$ = maximum velocity in the shock layer
U = vector of conserved properties in mean-flow equations
x,y = Cartesian coordinates
α = transformation variable defined by Eq. (1)
δ = boundary-layer thickness
ϵ = eddy viscosity coefficient
θ_ω = wedge angle
μ = molecular viscosity coefficient
ξ,η = skewed coordinates defined by Eq. (1)
τ_ω = wall shear stress

Introduction

BOUNDARY-layer separation from a surface upstream of a compression ramp with sufficiently large deflection has long been identified as an inviscid-viscous interaction problem. Interacting boundary-layer solutions over two-dimensional corners have been employed for laminar flows (see Refs. 1-3). More recently, an asymptotic solution on the identical subject also has been accomplished (Ref. 4). For all these solving schemes, either an iterative or a matching procedure must be implemented to accommodate simultaneously the shear stress dominant region and the associated inviscid stream. On the other hand, numerical solutions of the time-dependent Navier-Stokes equations have also been reported.[5-8] This direct approach automatically accomplishes the inviscid-viscous interaction. Crocco[9] indicates that the time dependency of the governing equations allows the solution to progress naturally from an initial guess to an asymptotic steady state. MacCormack developed a two-step difference method for solving the time-dependent Navier-Stokes equations and successfully investigated the interactions of a shock wave with a laminar boundary layer.[5] Recently, Baldwin and MacCormack[6] generalized the numerical scheme by including a turbulence model to analyze the turbulent interaction flowfield in the hypersonic regime. The flowfield structure of the shock impingement problem bears a close analogy to the flow over a compression corner. Carter[7] used the Brailovskaya finite difference scheme to study successfully, the laminar-flow separation over a compression corner. The first documented solution of turbulent flows on the compression ramp is probably due to Wilcox.[8] He adopted an explicit time-marching first-order finite difference scheme (AFTON 2pt code) with Saffman's turbulence model[10] to investigate two-dimensional separated turbulent flows. Comparisons of his numerical solutions and experimental data for the compression corner reveals substantial disparity. Wilcox offers two possible explanations for the discrepancy; first, the uncertainty of the two-dimensionality of the experimental data; and secondly, the eddy viscosity concept may be inappropriate, primarily due to the mean-flow streamline curvature. Nevertheless, one may hope that an improved turbulence model can be found. The present analysis utilizes the two-dimensional time-dependent Navier-Stokes equations as developed by MacCormack with an explicit finite differencing scheme[6] (alternating direction explicit). The concept of splitting reduces the set of two-dimensional equations into two sets of one-dimensional equations while retaining second-order accuracy. Cebeci-Smith's[11] eddy viscosity model provides the closure of the system of equations. The dependent variables thus degenerate into time-average properties of this fluid motion. It is well known that this composite algebraic eddy viscosity model is derived from the concept of an "equilibrium" turbulent boundary layer. The simple diffusive eddy viscosity model in

Presented as Paper 75-3 at the AIAA 13th Aerospace Sciences Meeting, Pasadena, California, January 20-22, 1975; submitted January 31, 1975; revision received April 25, 1975.

Index categories: Boundary Layers and Convective Heat Transfer—Turbulent; Jets, Wakes, and Viscid-Inviscid Flow Interactions; Supersonic and Hypersonic Flow.

*Aerospace Engineer, Flight Dynamic Laboratory. Member AIAA.
†Senior Scientist, Flight Dynamic Laboratory. Member AIAA.

its original form is incapable of explicitly, conveying any information about the history of this flowfield. The present investigation intends to improve on this characteristic to produce a relatively simple engineering tool. A simple but effective means will be to modify the eddy viscosity model to allow for a lag in the response of the turbulence to a sudden application of a severe adverse pressure gradient. In essence, the present analysis attempts to model a relaxation phenomenon within the aforementioned framework.

Two obvious objectives of the present effort can be summarized. The primary aspiration is to develop an engineering method capable of predicting turbulent-flow separation near a compression ramp. Substantiation of this approach and its range of validity is acquired through comparision with experimental data. Further understanding of this complicated turbulent-flow phenomenon is also planned, and hopefully the additional understanding may aid in the future development of turbulence modeling.

Governing Equations

The governing equations of the present analysis are the unsteady compressible Navier-Stokes equations in terms of mass-averaged variables. The adoption of the eddy viscosity coefficient and the turbulent Prandtl number reduces the conservation equations to the nearly identical form for laminar flows.[6] To avoid extensive interpolation of boundary conditions on the compression ramp, a skewed coordinate system is used. The relationship between the skewed and the Cartesian coordinate system is given by Carter[7] as

$$\xi = x \sec \alpha \tag{1a}$$

$$\eta = y - x \tan \alpha \tag{1b}$$

where

$$\alpha = \begin{cases} 0 & x \le x_c \\ \theta_\omega & x \ge x_c \end{cases}$$

The relating spatial derivatives of the coordinate system can be easily obtained as follows[7]

$$\partial/\partial x = \sec \alpha (\partial/\partial \xi) - \tan \alpha (\partial/\partial \eta) \tag{2a}$$

$$\partial/\partial y = \partial/\partial \eta \tag{2b}$$

One observes that the previous equations are valid for both of the straight segments of this compression ramp configuration. Carter[7] reveals that the derivative with respect to ξ requires special treatment to maintain second-order accuracy in the corner region. If one applies this spatial coordinate transformation, the two-dimensional mean-flow equations acquire the following expression

$$(\partial U/\partial t) + \sec\alpha(\partial F/\partial \xi) + (\partial G/\partial \eta) = 0 \tag{3}$$

The vector components are

$$U = \begin{Bmatrix} \rho \\ \rho u \\ \rho v \\ \rho e \end{Bmatrix} \tag{4}$$

$$F = \begin{Bmatrix} \rho u \\ \rho u^2 - \sigma_x \\ \rho uv - \tau_{xy} \\ (\rho e - \sigma_x) u - \tau_{xy}\, v - \gamma(\mu + \epsilon P_r/P_{r_t}) \\ \times \sec \alpha (\partial e_i/\partial \xi)/P_r \end{Bmatrix} \tag{5}$$

$$G = \begin{Bmatrix} \rho v - \rho u \tan \alpha \\ \rho uv - \tau_{xy} - \tan \alpha (\rho u^2 - \sigma_x) \\ \rho u^2 - \sigma_y - \tan \alpha (\rho uv - \tau_{xy}) \\ (\rho e - \sigma_y) v - \tau_{xy} u - \gamma (\mu + \epsilon \dfrac{P_r}{P_{r_t}}) \dfrac{\partial e_i}{\partial \eta} / P_r \\ -\tan\alpha [(\rho e - \sigma_x) u - \tau_{xy} v \\ -\gamma [\mu + \epsilon (P_r/P_{r_t})] \times (\partial e_i/\partial \xi)/P_r \end{Bmatrix} \tag{6}$$

Where the apparent stress components are given by

$$\sigma_x = -p - \tfrac{2}{3}(\mu+\epsilon)\left(\sec\alpha \frac{\partial u}{\partial \xi} - \tan\alpha \frac{\partial u}{\partial \eta} + \frac{\partial v}{\partial \eta}\right) + 2(\mu+\epsilon)\left(\sec\alpha \frac{\partial u}{\partial \xi} - \tan\alpha \frac{\partial u}{\partial \eta}\right) \tag{7}$$

$$\sigma_y = -p - \tfrac{2}{3}(\mu+\epsilon)\left(\sec\alpha \frac{\partial u}{\partial \xi} - \tan\alpha \frac{\partial u}{\partial \eta} + \frac{\partial v}{\partial \eta}\right) + 2(\mu+\epsilon)\frac{\partial v}{\partial \eta} \tag{8}$$

$$\tau_{xy} = \tau_{yx} = (\mu+\epsilon)\left(\frac{\partial u}{\partial \eta} + \sec\alpha \frac{\partial v}{\partial \xi} - \tan\alpha \frac{\partial v}{\partial \eta}\right) \tag{9}$$

The mean specific total energy is defined as:

$$e = c_v T + (u^2 + v^2)/2 \tag{10}$$

Auxiliary relationships included in the system of equations are the equation of state, perfect gas assumption, and Sutherland's viscosity equation. Upon the specification of the eddy viscosity model, molecular Prandtl number (0.72) and turbulent Prandtl number (0.90), the system of equations is completed.

The associated initial and boundary conditions are prescribed as follows: the initial conditions and upstream boundary conditions are prescribed for all the dependent variables. A detailed description of the upstream boundary condition will be deferred to the later section of the discussion. At the downstream boundary, gradients of all properties are assumed to vanish.[5,6]

$$\partial U/\partial \xi = 0 \text{ for } \xi \gg \xi_{\text{corner}} \tag{11a}$$

The outer boundary conditions for the present analysis consist of two regions, upstream and downstream of the coalescing waves. The former is satisfied by permitting the flow to approach its unperturbed freestream value

$$U(t,\xi,h) = U_\infty \tag{11b}$$

The region downstream of the coalescing shock system is fulfilled by the Rankine-Hugoniot relations

$$U(t,\xi,h) = U(M_\infty, \theta_\omega) \tag{11c}$$

The boundary conditions on the solid contour are given as

$$u(t,\xi,0) = 0 \quad v(t,\xi,0) = 0 \tag{11d}$$

$$T(t,\xi,0) = T_\omega \text{ (constant)} \tag{11e}$$

$$p(t,\xi,\Delta\eta) = p(t,\xi,-\Delta\eta) \tag{11f}$$

Diffusive Eddy Viscosity Model

From the viewpoint of engineering calculations, the compression ramp encounters severe difficulty, mainly arising

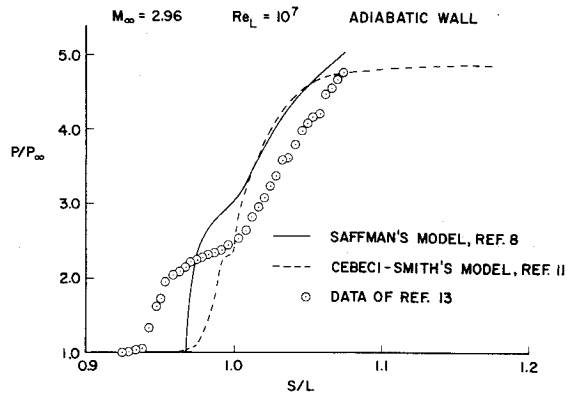

Fig. 1 Comparison of different turbulent models with experiment.

from the lack of knowledge concerning a fundamental representation of turbulence. In the corner region, the flow not only experiences a strong adverse pressure gradient, but also must negotiate a sharp corner. Bradshaw[12] in his work on the effects of streamline curvature on turbulent flows thoroughly discussed and summarized the various effects which could substantially alter the structure of turbulence. He also suggested several correction schemes to be used in the calculation methods. Uncertainty remains regarding the applicability of these corrections to the present problem.

Wilcox's numerical solution of separated turbulent flows resolve some of the unknowns. In short, the successfully demonstrates that the interacting turbulent flow inclusive of the separation phenomenon can be predicted by numercial analysis. His rate equation for turbulence in principle should be more suitable for interacting flows than the simple eddy viscosity model. The latter possesses no means of explicitly carrying any information about the history of the flowfield. For the sole purpose of comparison, a 25° compression ramp solution by Cebeci-Smith's eddy viscosty model is presented in Fig. 1, together with Wilcox's solution and the experimental data of Law.[13] It becomes obvious that neither turbulence model can produce an acceptable engineering solution, at least for the pressure distribution on the contour. The comparison is particularly poor in the initial phase of the intense interaction region. It should also be pointed out that this is the worst comparison of the six cases that Wilcox presented. The pronounced discrepancy in the leading portion of the pressure distribution seems to suggest a dramatic response of turbulence to the sudden adverse pressure gradient. Perhaps it reveals, as Bradshaw asserted,[12] that at supersonic Mach numbers, the effects of compression dominate over the effects of surface curvature.

Recently, several research efforts indicate that the Reynolds shear stress remains nearly frozen at its initial value and is convected along streamline in highly accelerated (or decelerated) flows.[14,15] The measurements[15] also indicate the Reynolds stress approaches a new equilibrium state exponentially. A reasonable explanation of this phenomenon has been given by Bradshaw.[12] He also suggests an empirical correction with a time scale corresponding to a streamwise distance of roughly 10 δ in the outer part of boundary layer. More recently, Rose and Johnson[16] also propose a similar formulation on the length scale to describe the history effects. Without more data on the relaxation phenomenon, one realizes it would be unrealistic to allow a complex correction. In this present analysis, the history effects are given by this following simple form

$$\epsilon = \epsilon_{\text{upstream}} + (\epsilon_{\text{equil}} - \epsilon_{\text{upstream}})\ [1 - \exp(-\Delta x/10\delta)] \quad (12)$$

Where $\epsilon_{\text{upstream}}$ is the calculated eddy viscosity coefficient at the initial locations of the pressure distrubance; ϵ_{equil} is the calculated local equilibrium value. The streamwise distance between these two locations is denoted by Δx. δ is the boundary-layer thickness at the initial station. The two-layer mixing length model of Cebeci and Smith[11] is described as follows. In the inner region

$$\epsilon_i = \rho k_1^2 y^2 D^2 \left| \frac{\partial q}{\partial \eta} \right| \quad (13)$$

where k_1 is the von Karman constant (0.4) and D is the Van Driest damping factor

$$D = 1 - \exp[-y(|\tau_\omega|/\rho_\omega)^{1/2}/26\nu_\omega] \quad (14)$$

In the outer region, Clauser's defect law gives

$$\epsilon_o = 0.0168\ \rho u_{\max} \delta^*_i \quad (15)$$

In the basic scaling, δ^*_i is the kinematic displacement thickness

$$\delta^*_i = \int_0^\infty \left(1 - \frac{u}{u_{\max}}\right) dy \quad (16)$$

Caution should be exercised to insure that once the switch is made from the inner value to the outer value, the calculation of eddy viscosity is restricted to Eq. (15). A modification is also required on the normalizing velocity $u_{\max}$ in Eq. (16) to prevent a possible numerical anomaly in the transient phase of the computations. More importantly, one must also appreciate that the outer edge of an intensely interacting boundary layer cannot be clearly defined. For this same reason, the intermittency correction in the law of the wake is also omitted. Technically, Cebeci-Smith's eddy viscosity model is generalized from a boundary-layer application to the Navier-Stokes flow regime.

Numerical Procedure

The present analysis adopts MacCormack's alternating-direction-explicit numerical scheme.[5] In the present version,[17] it contains two special procedures specially designed to eliminate several types of nonlinear instabilities. One is the averaging process, the other is the rather novel fourth-order product damping term in the predictor and corrector. The latter is essential for the analysis of flowfields with severe pressure gradients.

For the compression ramp configuration, the contour geometry is piecewise continuous. At present, no special treatment has been provided at the interface between the plate and the sharp wedge. According to Carter,[7] an interpolation process is required to maintain a second-order accurate solution. An improvement in numerical resolution is made possible by overlapping the computational domains. However, the overlapping capability also serves the purpose of providing an identical upstream boundary condition for all the subsequential inviscid-viscous interacting cases. The leading segment of the calculation domain is defined by a rectangle with the dimensions of 12×0.72 in. The height of the computational plane is roughly six times the boundary-layer thickness. Solutions in this region compare very well with calculations by an implict turbulent boundary-layer program developed previously.[18] The difference between the two solutions is within a few percent of both the skin-friction coefficient and velocity profile. All the necessary information is then stored at a given streamwise location to be used as the upstream boundary condition for the following corner region. On the compression ramp the computational region is defined by a trapezoid with the lower surface parallel to the wedge surface.

In the calculation, 64×22 computation mesh is employed. Grid spacing in the ξ direction is uniformly distributed for each computational domain. However, a different increment in ξ has been used for the leading plate ($\Delta\xi = 0.01695$ ft) and downstream of the overlapping location ($\Delta\xi = 0.00565$ ft).

The grid system consists of an exponentially varying inner region (16 points) and an equal-spacing outer region.[17] The finest step size in η is assigned to the viscous sublayer with a dimension of 10^{-4} ft.

The calculation is performed on a CDC 6600 digital computer. The rate of data processing is 0.028 sec per grid point for each time step. The evolution of dependent variables is monitored until the consecutive calculations indicate no significant change (0.1%), then the result is considered to be the asymptotic solution. A typical calculation requires about 300 time cycles (1½ hr) to achieve convergence.

Discussion of Results

Numerical results are presented in two groups. the first portion examines the feasibility of employing an eddy viscosity model with an empirical relaxation correction for predicting interacting turbulent flows with separation. The rest of the presentation is devoted to the verification of this concept through a comparison with experimental data. Before we proceed further in this discussion, clarification of the terminology is needed. In this present analysis, the "equilibrium" flow solution is defined as the calculation by means of the Cebeci-Smith eddy viscosity model. "Frozen" flow then is designated as the result obtained by holding the eddy viscosity coefficient profile constant at the undisturbed value upstream.

We have selected the location to be 0.929 ft from the leading edge of the flat plate for all cases computed. In principle, a sophisticated criterion can be utilized by freezing the eddy viscosity along a streamline as a function of the gradient. However, to demonstrate the cause and effect of relaxing the eddy viscosity, a more complicated model is not warranted at the present. The relaxation solution is described as the calculation with the eddy viscosity model given by Eq. (12). We emphasize that this eddy viscosity model is a similar version of that originated by Bradshaw[12] and Rose and Johnson.[16] They both propose a length scale adjustment on the eddy viscosity. The present correction only attempts to represent the flow history effect due to a strong compression, with no additional correction for the effects of streamline curvature, etc. incorporated.

In Fig. 2, the static pressure measurements of Law[13] along with three different numerical results are presented for the 25° compression ramp. The freestream Mach number is 2.96 and the Reynolds number based upon the leading plate length is 10^7. The equilibrium calculation fails completely in predicting the pressure variation in the corner region, in that it underpredicts the extent of the upstream propagation and produces a very short pressure plateau. In addition, the pressure approaches the inviscid asymptote at a more rapid rate than the experimental data indicates. The frozen solution on the other hand produces too large a separation region. The correct solution apparently is somewhere between these two extremes. A relaxation model employing Eq. (12) produces a

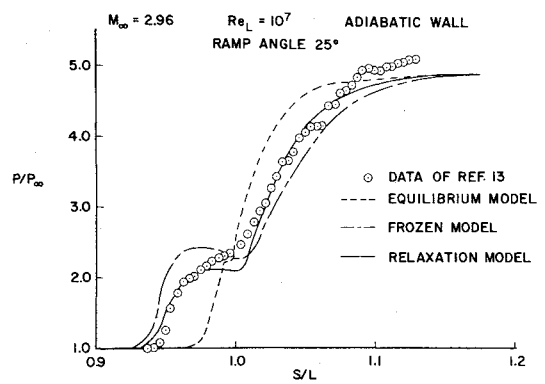

Fig. 2 Pressure distribution for equilibrium, frozen, and relaxation eddy viscosity models.

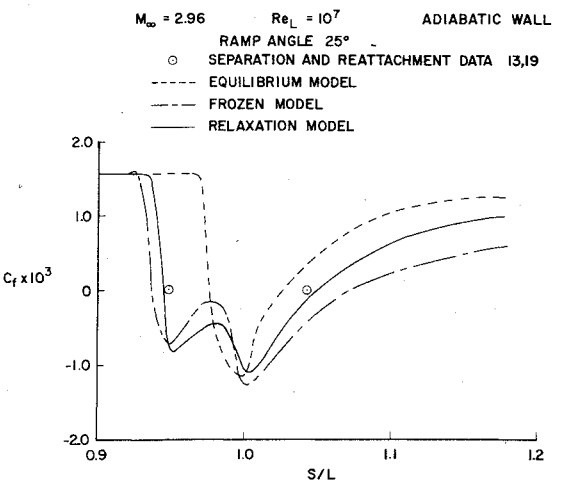

Fig. 3 Skin friction coefficient distributions for equilibrium, frozen, and relaxation eddy viscosity models.

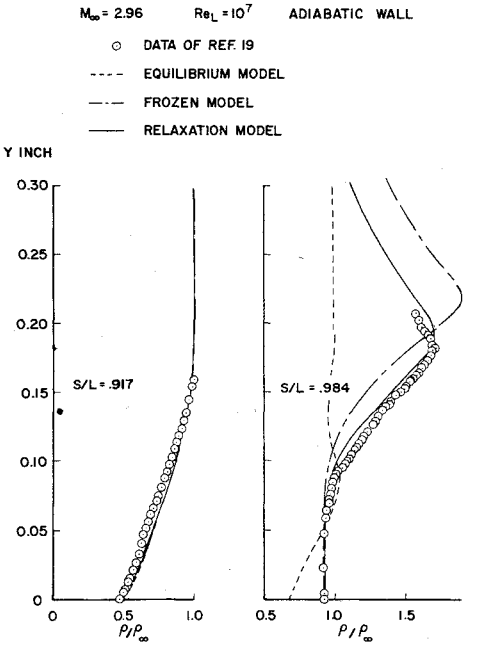

Fig. 4 Density profiles for equilibrium, frozen, and relaxation eddy viscosity models.

solution with marked improvement over the two aforementioned calculations. Significant discrepancy between the data and the present calculation only appears in the pressure plateau, near the corner.

The calculated skin-friction coefficient distributions are present in Fig. 3. The striking feature of this presentation is the drastic difference in the shear stress distributions for the three calculations. The difference is perhaps anticipated in view of the three substantially different surface pressure variations. Interestingly enough, the unusual dual-minimum skin-friction distribution is also encountered for laminar flows with extensive separation region.[1-4] Unfortunately, no experimental skin-friction data are available for this case, however, oil flow measurements indicated the separation and reattachment points of the flow. The relaxation calculation exhibits an excellent comparison with the experimental data. The discrepancy between data and numerical result is within a fraction of the boundary-layer thickness. However, the equilibrium and the frozen calculations significantly under- and over-predict these locations, respectively. In short, the present relaxation scheme seems able to predict adequately the important engineering features of the ramp problem. Then it would be logical to seek further verification of the present assertions in the prediction of detailed flowfield properties.

In Fig. 4, we present a comparison between the measured

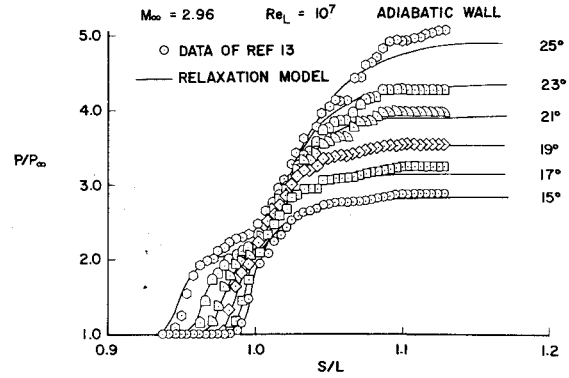

Fig. 5 Pressure distributions for various compression ramp angles.

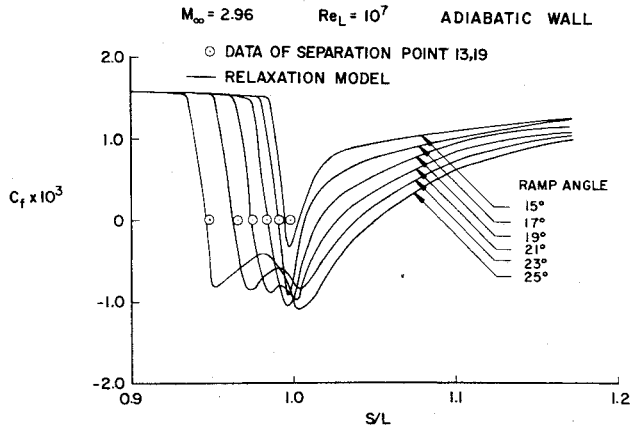

Fig. 6 Skin friction coefficient distributions for various compression ramp angles.

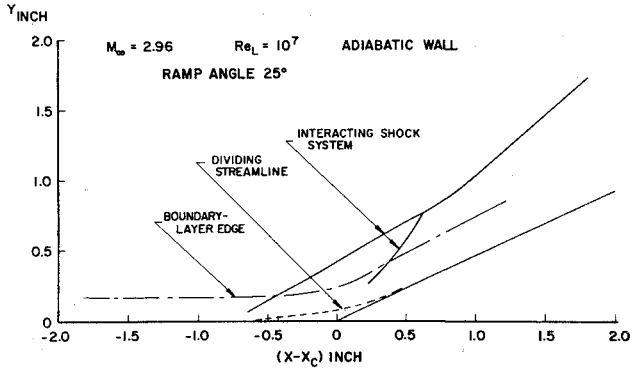

Fig. 7 Computed flowfield structures for a 25° compression ramp.

Fig. 8 Interferogram for the flow over a 25° compression ramp.

and calculated density profiles at two streamwise locations. The experimental data are direct measurements from an interferogram by means of evaluating the fringe shifts.[19] The affinity between data and the relaxation calculations upstream and in the separated flow region is obvious.

Encouraged by these results, a series of calculations was performed in an attempt to establish the range of validity of the relaxation eddy viscosity model. The investigated ramp angles span a range of 15-25° at an interval of 2° apart. The computed surface pressure distributions together with the corresponding experimental data[13] are given in Fig. 5. In general, the difference between the data and the numerical results is small. Excellent predictions of the pressure propagation upstream of the corner have been achieved. Significant discrepencies between the data and the calculations appear only in the corner region for the high ramp angle (Fig. 2).

The skin-friction coefficient distributions for the compression ramp at six different ramp angles are presented in Fig. 6. Experimental data,[13,19] of this separation location (using several techniques) for different ramp angles are also provided in this graph. For the 15° ramp, the calculations indicate a very small region of separation with a dimension less than ⅔ of the boundary-layer thickness. The corresponding experimental observation reveals even a small region of the separated flow. In general, the calculations predict accurately the point of separation. For all the investigated cases, the predictions are well within the data scatter band of the different experimental techniques. In this graph, one observes a systematic evolution of the skin-friction coefficient from a single-minimum distribution into a dual-minima behavior as the separation domain increases substantially. This trend has also been observed for separated laminar flows.[1-4]

The preceding results offer support of a relaxation eddy viscosity model for performing engineering calculations. We will devote the rest of the presentation to delineate the significant characteristics of interacting separated turbulent flows.

In Fig. 7, the complete interacting flowfield, including the separation phenomenon, is presented. The experimental data are obtained chiefly from the optical and oil-flow studies of the 25° ramp configuration by Havener, and Radley[19] and Law.[13] Upstream of the corner a clearly defined outer edge of the turbulent boundary layer can be discerned. The normal velocity component in the boundary layer first reveals significant adjustment in magnitude, then exhibits a rapid pressure rise in the wall region as the corner is approached. Adjacent to the separation point, the coalesence of compression waves is evident. The penetration of the separation induced shock wave reaches the shear stress dominated inner region. The order-of-magnitude difference between the two velocity components diminishes in the outer portion of the shear layer. Extensive spearation is located around the corner; the boundary-layer growth increases rapidly but still reveals a clearly identifiable outer edge. Further downstream of the corner, a second coalescing shock wave at reattachment also becomes detectable. The second shock eventually intersects the leading separation shock, producing an obvious change in the slope of the wave front. Downstream of this intersection point, no distinctive outer edge of the boundary layer can be clearly defined. Instead, a rotational field produces a streamwise velocity gradient. The numerical result essentially duplicates the experimental observations (Fig. 8).

The comparison of the density profiles at several streamwise locations between the data and calculation is presented in Fig. 9. The data are directly evaluated from the fringe shifts;[19] therefore, this outer limit of data either represents the encountering of a shock wave or a uniform-flow region. All the data and calculated density profiles are presented in the coordinate perpendicular to the surface. Interpolation of the computed results downstream of the corner is required to

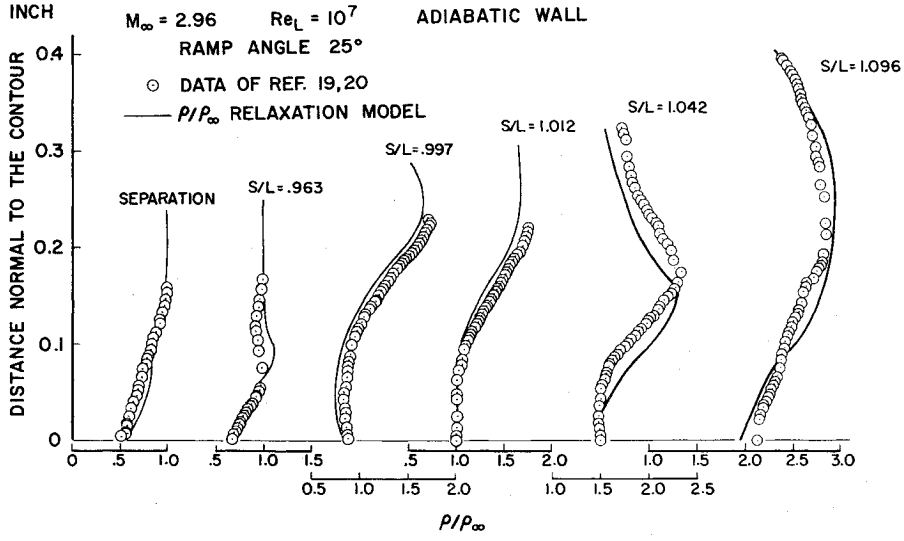

Fig. 9 Density profiles for a 25° compression ramp.

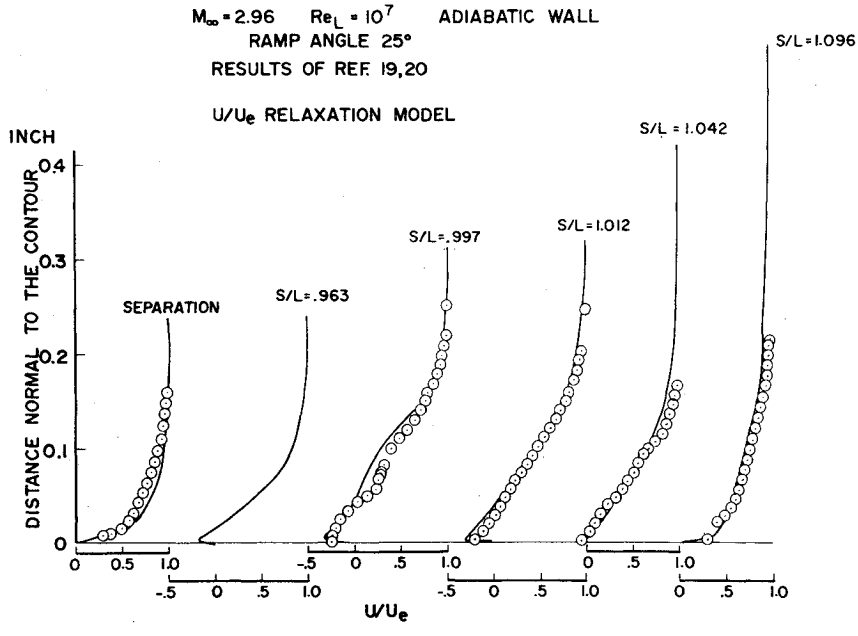

Fig. 10 Velocity profiles for a 25° compression ramp.

present the information in this format. In general, the numerical results predict the measured density profiles within a few per cent.

In the last graph (Fig. 10), we present several streamwise velocity profiles in the body orientated coordinates. One observes a sequence of turbulent boundary layers through this interaction region which separates, reattaches, and finally exits as a confined shear layer. Havener, and Radley also deduced several velocity profiles from their optical measurements.[19,20] They obtained the velocity data through the Crocco relationship and by linearly interpolating the pressure across the boundary layer. The comparison between the data and the calculation reveals good conformity throughout.

Conclusions

Although excellent agreement has been obtained between experimental data and numerical calculations for turbulent flows with zero pressure gradient, all turbulence models (either the eddy viscosity model[18] or the more sophisticated model equations[10] fail to predict turbulent flows with strong adverse pressure gradients. In the present analysis, a simple but effective modeling of the turbulence response to a suddenly applied pressure gradient has been incorporated into an eddy viscosity model. The modifications reproduce the relaxation phenomenon of turbulence by adopting an exponential decay of the unperturbed eddy viscosity with a characteristic length scale.

The relaxation eddy viscosity model is combined with the Navier-Stokes equations to form a closed system of equations. The results demonstrate that the turbulence model adequately predicts the inviscid-viscous interacting turbulent flow, including the separation phenomenon. The comparisons with experimental data of Law,[13] Havener and Radley[19] for compression ramps indicate that the present method accurately predicts the upstream pressure propagation and location of the separation and reattachment points. A very good resolution on the detailed flowfield variables is also accomplished.

References

[1] Dwoyer, D. L., "Supersonic and Hypersonic Two-Dimensional Laminar Flow over a Compression Corner," *Proceedings of AIAA Computational Fluid Dynamics Conference*, July 1973, Palm Springs, Calif.

[2] Werle, M. J. and Vatsa, V. N., "Numerical Solution of Interacting Supersonic Boundary Layer Flows Including Separation Effects," ARL 73-0162, Aerospace Research Labs., Wright-Patterson AFB, Ohio, Dec. 1973.

[3] Holden, M. S., "Theoretical and Experimental Studies of Laminar-Flow Separation on Flat Plate-Wedge Compression Surfaces in the Hypersonic Strong Interaction Regime," ARL 67-0112, Aerospace Research Labs., Wright-Patterson, AFB, Ohio, May 1967.

[4] Jensen, R., Burggraf, O. R., and Rizzetta, D. P., "Asymptotic Solution for Supersonic Viscous Flow Past a Compression Corner," *Lecture Notes in Physics*, Vol. 35, Springer-Verlag, New York, 1975, pp. 218-224.

[5] MacCormack, R. W., "Numerical Solutions of the Interaction of a Shock Wave with a Laminar Boundary Layer," *Lecture Notes in Physics*, Vol. 8, Springer-Verlag, New York, 1971, pp. 151-163.

[6] Baldwin, B. S. and MacCormack, R. W., "Numerical Solution of the Interaction of a Strong Shock Wave with a Hypersonic Turbulent Boundary Layer," AIAA Paper 74-558, Palo Alto, Calif., 1974.

[7] Carter, J. E., "Numerical Solution of the Supersonic Laminar Flow over a Two-Dimensional Compression Corner," *Lecture Notes in Physics*, Vol. 19, Springer-Verlag, New York, 1973, pp. 69-78.

[8] Wilcox, D. C., "Numerical Study of Separated Turbulent Flows," AIAA Paper 74-584, Palo Alto, Calif., 1974.

[9] Crocco, L., "A Suggestion for the Numerical Solution of the Navier-Stokes Equations," *AIAA Journal*, Vol. 3, Oct. 1965, pp. 1824-1832.

[10] Saffman, P. G. and Wilcox, D. C., "Turbulence Model Predictions for Turbulent Boundary Layer," *AIAA Journal*, Vol. 12, April 1974, pp. 541-546.

[11] Cebeci, T., Smith, A. M. O., and Mosinskis, G., "Calculations of Compressible Adiabatic Turbulent Boundary Layer," *AIAA Journal*, Vol. 8, 1970, pp. 1974-1982.

[12] Bradshaw, P., "Effects of Streamline Curvature on Turbulent Flow," AGARDograph No. 169, (AGARD-AG-169), Aug. 1973.

[13] Law, C. H., "Supersonic, Turbulent Boundary-Layer Separation," *AIAA Journal*, Vol. 12, June 1974, pp. 794-797.

[14] Deissler, R. G., "Evolution of a Moderately Short Turbulent Boundary Layer in a Severe Pressure Gradient," *Journal of Fluid Mechanics*, Vol. 64, Part 4, 1974, pp. 763-774.

[15] Narasimha, R and Prabhu, A., "Equilibrium and Relaxation in Turbulent Wakes," *Journal of Fluid Mechanics*, Vol. 54, Part 1, 1972 pp. 1-17.

[16] Rose, W. E. and Johnson, D. A., "A Study of Shock-Wave Turbulent Boundary-Layer Interaction Using Laser Velocimeter and Hot-Wire Anemometer Techniques," AIAA Paper 74-95, Washington, D. C., 1974.

[17] MacCormack, R. W., "Numerical Methods for Hyperbolic Systems," Lecture Notes for short course on Advances on Computational Fluid Dynamics. University of Tennessee Space Institute, Tullahoma, Tenn., Dec. 10-14, 1973.

[18] Shang, J. S., Hankey, Jr., W. L., and Dwoyer, D. L., "Numerical Analysis of Eddy Viscosity Models in Supersonic Boundary Layers," *AIAA Journal*, Vol. 11, Dec. 1973, pp. 1677-1683.

[19] Havener, A. G. and Radley, R. J., "Turbulent Boundary-Layer flow Separation Measurements Using Holographic Interferometry," *AIAA Journal*, Vol. 12, Aug. 1974, pp. 1071-1075.

[20] Havener, A. G. and Radley, R. J., "Supersonic Wind-Tunnel Investigations Using Pulsed Laser Holography," ARL 73-0148, Oct. 1973, Aerospace Research Labs., Wright-Patterson AFB, Ohio.